

# Numerical Simulation of Hydraulic Shock in a Water Pumping System Protected by Air

ANCA CONSTANTIN , CLAUDIU STEFAN NITESCU  
Hydraulic Engineering Department , Faculty of Civil Engineering  
"Ovidius" University  
Constanta, 22B Unirii Str.  
ROMANIA

[aconstantina@univ-ovidius.ro](mailto:aconstantina@univ-ovidius.ro), [http://www.univ-ovidius.ro/faculties/civil\\_eng](http://www.univ-ovidius.ro/faculties/civil_eng)

*Abstract:* - Air may be efficiently used in water pumping system protection from hydraulic shock, due to its elasticity. The paper presents the results regarding the extreme pressures in the discharge duct of a pumping installation, obtained by numerical simulation of the water hammer phenomenon in two cases of protection with air: using air chamber and using free air dispersed throughout the pumped water. The air chamber increases the pipe wall elasticity in the particular section where the chamber is mounted. The air bubbles transform single-phase water into a biphasic fluid with greater compressibility. Specific parameters are related to these methods, in order to establish criteria for best protection solution choice in water supply engineering design.

*Key-Words:* - Hydraulic Shock, Pumping Installation, Air Chamber, Biphasic Flow, Dissolution.

## 1 Introduction

The engineering design of a pumping installation aims to achieve the requested discharge and head at an optimal energetic efficiency, and also to prevent operation instabilities and damaging phenomena such as cavitation and water hammer. Our study focuses on a water pumping installation and two of the ways of protection from hydraulic shock: by air chamber and by free air dispersed in pumped water. The air chamber locally offers elasticity to the conduit due to air compressibility [7], [14]. The presence of small amounts of free air in the water results in a smaller celerity, due to the change of density of the biphasic fluid. In the engineering design, the choice of one or the other of these protection solutions must be theoretically studied. There must be known their efficiency and limitation.

Numerical simulation, using specially written or commercial computer programs, is the most reliable and low cost method of comparative study.

## 2 Pumping Installation Protection from Water Hammer

The hydraulic shock is one of the most damaging phenomena in a water supply system. Therefore, the specialists in hydraulics and mathematicians have been paying their attention to the rigorous study of the water transient movement in closed conduits. The hydraulic shock may occur in a pumping installation equipped with  $N$  pumps mounted in parallel, in three main cases:

when the first pump is turned on, when the last pump is turned off and, the most dangerous case, when all the pumps accidentally stop due to a power failure.

There have been conceived different methods to solve the hydraulic shock problems, such as: arithmetic water hammer, graphical water hammer, algebraic method, characteristics method, miscellaneous methods based on the linearization of the differential equations [7], [9], [14].

We may also mention a series of devices conceived and designed to protect tubes from the threat of water hammer: surge tank, air chamber, water chamber, asymmetrical flow resistance device etc. [10].

Air chamber is frequently used in practice. In engineering design, the dimensioning of such a device is carried out according to the recommendation that the ratio air volume to total chamber volume has to be approximately 0,3. There are no references with respect to the air volume decrease by dissolution in water inside the air chamber. There were reported some accidents in pumping installations equipped with air chamber mounted on the discharge duct, when the air volume hadn't been monitored for a long period of time [5]. In these cases, the pressure values reached during water hammer were greater than the ones recorded in the absence of the air chamber.

Free air dispersed into the pumped water is a more recently conceived method. The biphasic flow inside the pipeline is rather complex, therefore this method has been studied assuming simplifying hypotheses [2]. The free air may be deliberately introduced in the discharge

duct using a compressor, which allows a rigorous control on the air flow rate. The influence of air on the wave propagation speed is depicted in [2], [5], [10]. We are interested in further information regarding extreme pressure during hydraulic shock and the range of air volume fraction in which this method is efficient.

### 3 Case Study

#### 3.1 Hydraulic Shock Equations

The installation we focused on is equipped with a double flux centrifugal hydraulic pump, type 12NDS. The operation point is given by the discharge  $Q = 0.106 \text{ m}^3/\text{s}$  at the head  $H = 14 \text{ m}$ . The steel made discharge duct is horizontally mounted. It has  $500\text{m}$  in length and a diameter of  $300 \text{ mm}$ . The layout of the installation is shown in Fig.1. Water is pumped at a geodetic height of  $9\text{m}$ . The discharge duct is equipped with a check valve that prevents water from flowing back in an accidentally pump stoppage situation. In fact, this type of stoppage is taken into account as the source of perturbation in our discussion.

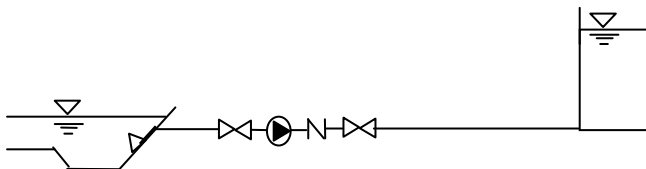


Fig.1. Pumping installation with horizontal discharge duct

Our purpose is to determine the best solution of protection from hydraulic shock for this installation, considering the air chamber method versus the free air method. Consequently, there were determined, by numerical simulation, the extreme pressures in the discharge duct, in the section next to the pump, during water hammer, in three hydraulic shock situations: when the pipeline is not protected by any devices (as the reference case), when the discharge duct is protected by an air chamber mounted next to the pump and when free air is homogeneously spread into the pumped water by the help of a compressor. Further more, we envisage finding out the range of efficient protection for each method, considering the following parameters:

- the ratio of air volume to chamber volume,  $\beta$ ;
- the volume fraction of free air in the biphasic mixture,  $\alpha$ .

The pressure variation in the discharge duct was simulated by the program *Hammer*. The mathematical model used for the water hammer phenomenon assumes that the water flows in a single direction (along the longitudinal axis of the pipe) and the head losses may be calculated using the same formulas as in the steady

regime. The main equations are the momentum conservation equation (1):

$$\frac{\partial H}{\partial x} + \frac{1}{g} \frac{\partial v}{\partial t} + \frac{\lambda}{2gD} v|v| = 0 \quad (1)$$

and the continuity equation (2):

$$\frac{\partial H}{\partial t} + \frac{c^2 \partial v}{g \partial x} = 0 \quad (2)$$

where:  $v$ -velocity, [m/s];

$H$ -head, [m];

$c$ -celerity, [m/s];

$D$ -pipe's diameter, [m];

$\lambda$ -Darcy's coefficient;

$g$ -gravitational acceleration,  $g = 9,81 \text{ m/s}^2$ .

The term  $\frac{\lambda}{2gD} v|v|$  in equation (1) stands for the head losses on pipe's length unit, calculated with Darcy's formula [5]. This term may be neglected only for the first water oscillation. For the subsequent oscillations, it contributes to the water oscillation damping.

The characteristics method is the most used in numerical simulation of the hydraulic shock, due to its precise results, even in solving complex system problems. It allows a relative easy implementation of various boundary conditions.

The characteristics method transforms the partial differential equations (1) and (2) into four total differential equations, knowing that  $v \ll c$ :

$$\frac{dx}{dt} = \pm c \quad (3)$$

$$\pm \frac{g}{c} \frac{dH}{dt} + \frac{dv}{dt} + \frac{\lambda}{2D} v|v| = 0 \quad (4)$$

The sign "+" stands for the direct wave and the sign "-" for the indirect wave. In current technical problems the celerity is constant for a given duct, consequently the relations (3) represent straight lines along which the relations (4) are compatible. The method is clearly explained in detail in [10], [14]. The equation system can be solved by a finite-difference technique. Written in finite differences the main equations governing the hydraulic shock become the velocity equation (5):

$$v_{j,t+\Delta t} = \frac{1}{2} \left[ v_{j-1,t} + v_{j+1,t} + \frac{g}{c} (H_{j-1,t} - H_{j+1,t}) \right] - \frac{\lambda}{2} \quad (5)$$

and the head equation (6):

$$H_{j,i+1} = \frac{1}{2} \left[ H_{j-1,i} + H_{j+1,i} + \frac{c}{g} (v_{j-1,i} - v_{j+1,i}) - \frac{c}{g} \right] \quad (6)$$

where: subscript  $i$  accounts for time,  
 subscript  $j$  accounts for node,  
 $\Delta t$ -step of time, [s].

The studied duct is divided into sections and the equations (5) and (6) allow the calculation of speed and head in each node, knowing the initial regime conditions.

Specific relationships are added to these equations according to the envisaged type of water hammer protection of the discharge pipe.

### 3.2 Protection with Air Chamber

#### 3.2.1 Specific Hydraulic Shock Equations

Specific boundary conditions are imposed for the upstream and downstream end of the duct and for the node where the air chamber is mounted. These conditions result in additional equations written also in finite differences.

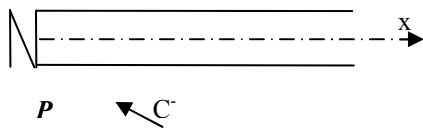


Fig.2. Upstream end of the discharge duct. Node  $P$  with check valve

At the upstream end of the duct, Fig.2, the boundary conditions are imposed by the check valve clothing. The closing law allows the determination of  $v_{j,i+1}$ . The head  $H_{j,i+1}$  results as [10]:

$$H_{P,i+1} = H_{P+1,i} + \frac{c}{g} (v_{P,i+1} - v_{P+1,i} + \frac{\lambda \Delta t}{2D} v_{P+1,i}) \quad (7)$$

At the downstream end of the duct, there is an open reservoir with constant head, Fig. 3. Therefore:

$$H_{N,i+1} = H = \text{const} \quad (8)$$

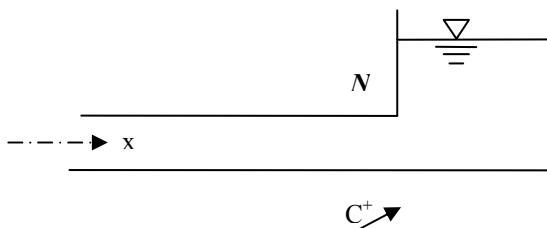


Fig.3. Downstream end of the discharge duct. Node  $N$  with constant head reservoir

$$v_{N,i+1} = v_{N-1,i} - \frac{g}{c} (H_{N,i+1} - H_{N-1,i}) - \frac{\lambda \Delta t}{2D} v_{N-1,i} \quad (9)$$

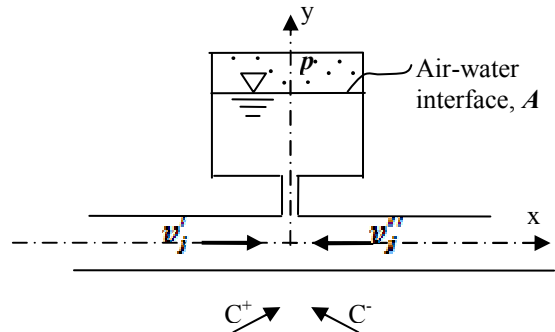


Fig.4. Node with air chamber

It was assumed that the discharge duct is equipped with an air chamber of total volume  $V_a = 4m^3$  as it may be seen in Fig.4. The equations (10)-(12) are specific for a calculus node with an air chamber [10], assuming a polytropic process for air.

$$H_{i,i+1} = y_{j,i+1} + \frac{p_{j,i+1}}{\gamma} \quad (10)$$

$$p_{j,i+1} V_{j,i+1}^n = p_{j,i} V_{j,i}^n \quad (11)$$

$$V_{j,i+1} = V_{j,i} + A(v_{r,i+1} + v_{r,i}) \frac{\Delta t}{2} \quad (12)$$

where  $p$ -air pressure, in the air layer inside the chamber,  $[N/m^2]$ ;

$V$ - volume of air in the chamber,  $[m^3]$ ;

$v_r$ -ascensional velocity of water surface level in the air chamber,  $[m/s]$ ;

$n$ -polytropic exponent;

$y$ -elevation of water surface in the air chamber,  $[m]$ ;

$A$ -air-water interface area,  $[m^2]$ .

The celerity in a water pipeline depends both on water compressibility and pipe wall elasticity [3], [5], [9]. The relation (13) stands for celerity in a single liquid phase, taking into account the elastic behaviour of the pipe wall:

$$c = \left(\frac{E_i}{\rho_i}\right)^{1/2} \left(1 + \frac{E_i D}{E_c e} k\right)^{-1/2} \quad (13)$$

where  $\rho_i$ -water density, [ $kg/m^3$ ];

$E_i$ -modulus of elasticity of water, [ $N/m^2$ ];

$E_c$ -modulus of elasticity of the pipe wall, [ $N/m^2$ ];

$e$ -pipe-wall thickness, [ $m$ ];

$k$ -coefficient depending on the pipe's emplacement.

There was assumed a constant celerity along the pipeline.

### 3.2.2 Model for Air Dissolution in Water

A problem encountered in pumping stations exploitation, in the case the air chamber isn't monitored for a long time, is the decrease of the compressed air volume by the air dissolution in water. The phenomenon is more intense in the systems with large aria air-water interface and high air pressure.

Dissolution of compressed air into the water, inside the chamber may change the ratio of the volume of air to the total volume of the reservoir:

$$\beta = \frac{V}{V_r} \quad (14)$$

where  $V_r$ - total volume of chamber, [ $m^3$ ].

An evaluation of the air volume rate absorbed in the water is possible considering the transport equation of the gas. We assumed air to be single sort of perfect gas. In the absence of any chemical reaction between the two fluids, the transport equation is [2], [15]:

$$\frac{\partial C}{\partial t} + \nabla \cdot (-D_{aw} \nabla C) + \vec{u} \cdot \nabla C = 0 \quad (15)$$

where  $D_{aw}$ -diffusion coefficient of air in water, [ $m^2/s$ ];

$\vec{u}$ - velocity, [ $m/s$ ].

$C$ - concentration of air dissolved in water, [ $mol/m^3$ ];

Both fluids are at rest inside the chamber, so the convective term in equation (15) equals zero. The equation (15) becomes:

$$\frac{\partial C}{\partial t} + \nabla \cdot (-D_{aw} \nabla C) = 0 \quad (16)$$

We considered that pressure  $p$  in the air layer inside the chamber remains constant, which allowed us to impose a constant concentration at the air water interface, determined by the use of Henry's law [13]:

$$C_s = \frac{p}{X} \quad (17)$$

where  $p$ - air pressure in the chamber, [ $N/m^2$ ];  
 $X$ --Henry's constant, [ $Pa \cdot m^3/mol$ ];

We also assumed a constant concentration in the inferior section of the chamber, where water in the chamber is adjacent to water in the discharge duct.

Considering that concentration of air in water varies only on the y axis of the chamber, Fig.4, we obtained by integration, with Dirichlet boundary conditions, the concentration variation as showed in Fig.5.

The normal diffusive flux of air (expressed on unit of length) through the inferior section of the chamber towards the protected discharge duct is represented in Fig.6. It exponentially varies in time. It may be noticed that the water in the chamber becomes saturated after a week. Thus, after this period we may assume a steady state for the mass transfer.

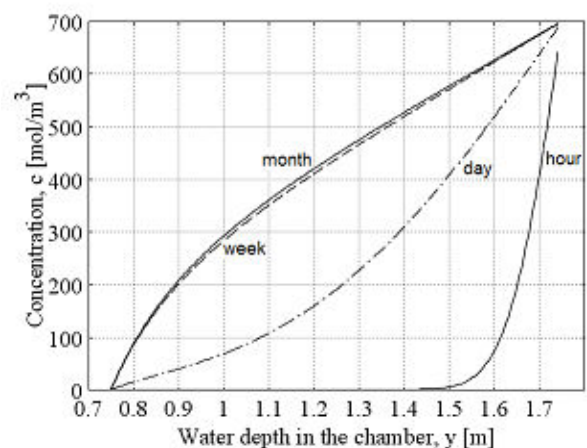


Fig.5. Variation of air concentration in water, inside the chamber, for different exposure times

Taking into account the dimensions of the section, the flux tends to a constant value,  $\varphi = 5,2 \cdot 10^{-5} mol/m^2 \cdot s$ .

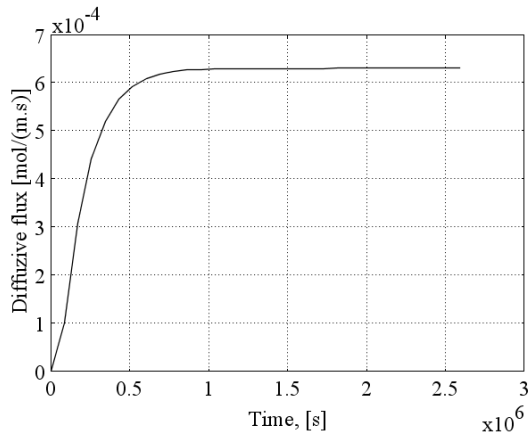


Fig.6. Air diffusive flux on unit of length, at the inferior section of the chamber, towards the water in the discharge duct

The mass flow rate transferred between the two phases, in steady state, is depicted by the relationship:

$$\dot{m}_{aw} = \dot{\phi} \cdot M \cdot A \tag{18}$$

where  $\dot{m}_{aw}$ -mass flow rate transferred between air and water, [ $kg/s$ ];

$M$ -equivalent molecular weight of air, [ $kg/mol$ ].

The equivalent molecular weight of air,  $M$ , the equivalent Henry's constant,  $X$ , and the diffusivity coefficient,  $D_{aw}$ , were calculated as weighted averages of the oxygen and nitrogen correspondent properties, assuming air to be a perfect gas composed only of the two mentioned gases [2].

The mass flow rate value determined with the relation (18) allows us to determine the volume flow rate of air, at constant temperature and pressure.

$$\dot{V} = \frac{\dot{m}_{aw} \cdot R \cdot T}{p} \tag{19}$$

where  $R$  -air constant, [ $J/(kg \cdot K)$ ];

$T$  -absolute temperature, [ $K$ ];

### 3.3 Protection with Free Air

The model used to simulate the hydraulic shock in the case of free air protection assumed a homogenous air-water mixture, where water was the continuous phase and the air the dispersed one.

The mathematical model is the same used for the air chamber protection (except for the specific equations referring to the calculus node with chamber), but celerity is calculated with a modified relationship [3], as follows. We assumed the flow of the biphasic fluid was homogenous, that means the velocity for gas is equal to the water velocity [2], [11]. Both phases are subjected to the same pressure field.

Taking into account a control volume  $V_a$  filled with biphasic fluid, the volume fraction of air  $\alpha$ , is defined by the ratio:

$$\alpha = \frac{V}{V_a} \tag{20}$$

A similar volume fraction might be written for water  $\alpha_l$ :

$$\alpha_l = \frac{V_l}{V_a} \tag{21}$$

Thus, the relationship between the two volume fractions becomes [2]:

$$\alpha_l = 1 - \alpha \tag{22}$$

The presence of air bubbles modifies the parameters of fluid [8]. So, instead of considering the water density, the density of the biphasic fluid,  $\rho_m$ , was taken into account. The biphasic fluid density may be expressed using the volume fractions [2]:

$$\rho_m = \rho_l \alpha_l + \rho_a \alpha \tag{23}$$

The term related to the air density may be neglected. Consequently, the mixture density will be:

$$\rho_m = \rho_l \left( 1 - \frac{m_a RT}{p} \right) \tag{24}$$

The new expression of the density leads to the following form for the celerity relationship: [5]

$$c_a = \left( \frac{E_l}{\rho_l} \right)^{1/2} \left[ \left( 1 - \frac{m_a RT}{p} \right) \cdot \left( 1 + \frac{m_a RT}{p^2} \cdot E_l + \frac{E_l l}{E_c \epsilon} \right) \right] \tag{25}$$

where- $m_a$  -air mass on biphasic unit volume, [ $kg/m^3$ ].

Assuming the air mass on biphasic unit volume to be constant, that means the air dissolution and liberation are neglected (no mass transfer between bulk water and air bubbles), the term  $\frac{m_a RT}{p^2} \cdot E_l$  has an important weight on

celerity at small pressures. This term may be neglected at pressures exceeding 40 bar [5].

## 4 Results

The numerical simulation of the hydraulic shock in the specified pumping discharge duct was achieved by the use of a special computer program, based on the mathematical model of the water hammer phenomenon written in finite differences and solved by the method of characteristics.

The numerical simulation for the hydraulic shock in the given installation was carried out in the following circumstances:

*a.* the pipeline is not provided with any protection device;

*b.* the pipeline is equipped with an air chamber and the ratio  $\beta$  drops from 0,75 to 0,025;

*c.* the pipeline hasn't any protection device, but free air is continuously introduced by the help of a compressor, right downstream the pump; the air volume fraction  $\alpha$  is rigorously varied from 0,5 to 10 %.

In order to compare the extreme pressures obtained in the above mentioned cases during hydraulic shock, the variation of pressure is graphically represented for the same cross section of the discharge duct, next to the pump.

### 4.1 Pipeline without Protection from Water Hammer

In the case of no protection, the extreme values of pressure may be seen in Fig. 7. Maximal pressure reaches 132 mwc, value that might be dangerous for an installation conceived to resist at maximum 10 bar.

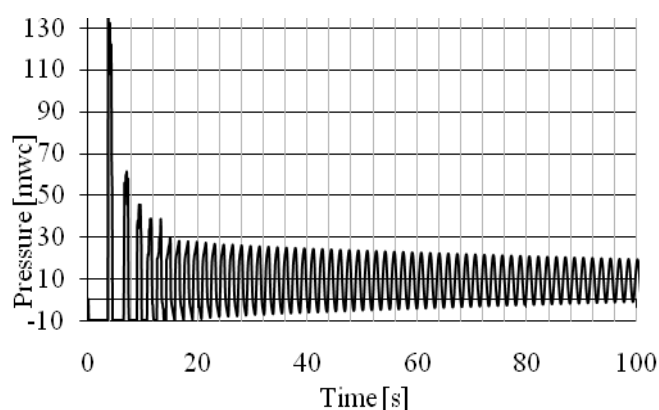


Fig.7. Pressure variation in the unprotected conduit

Cavitation occurs during the first 20s of the unsteady movement.

### 4.2 Pipeline Protected by Air Chamber

In the second case, when the duct is protected by an air chamber, the maximal pressure in the same node decreases very much for  $0,75 \geq \beta \geq 0,3$ , Fig.8. The pressure rises only to 28mwc.

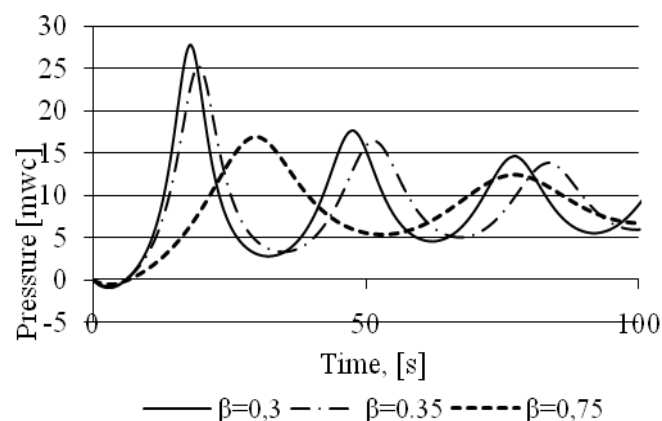


Fig.8 Pressure variation in the case of the discharge duct protected by air chamber; large air volume in the chamber

When the ratio range is  $0,3 > \beta \geq 0,2$  the air chamber still works as a protection device, but is less efficient. After the first 5 seconds, time for the check valve to close, negative pressure inside the duct disappears. Fig.9 shows that a decrease with 5% of the ratio  $\beta$  (from 0,15 to 0,1) results in a decrease of the maximal pressure with about 20 mwc.

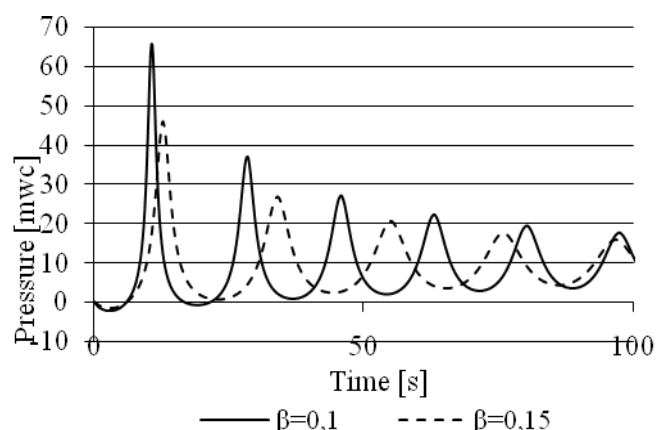


Fig.9 Pressure variation in the case of the discharge duct protected by air chamber; medium air volume in the chamber

The maximal pressure rises up to larger values as  $\beta$  continues to decrease.

Finally, if the air volume isn't monitored and reaches the value  $\beta = 0,025$ , the air chamber becomes a threat to the duct, because the maximal pressure reaches 160mwc, greater than the correspondent value in the case when there are no protection means for the duct. Pressure variation in the case of such small air volumes in the chamber is graphically represented in Fig. 10.

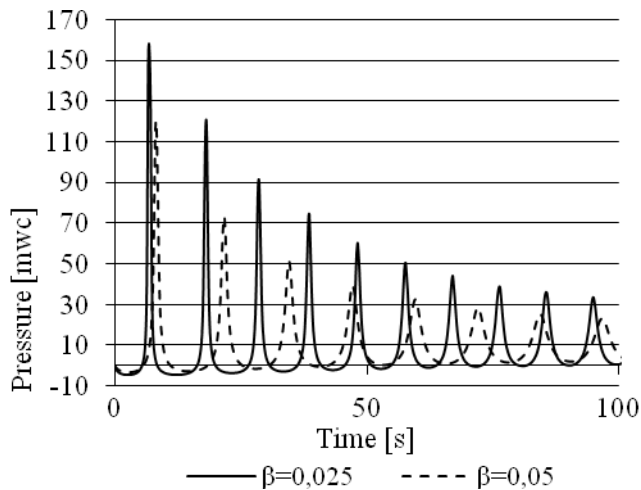


Fig.10. Pressure variation in the case of the discharge duct protected by air chamber; small air volume inside the air chamber

The decrease in time of ratio  $\beta$ , due to air dissolution in water, was represented in Fig.11. The volume flow rate of absorbed air was determined from the mass flow rate  $\dot{m}_{aw}$  given by the relationship (12), at a temperature of 15 °C.

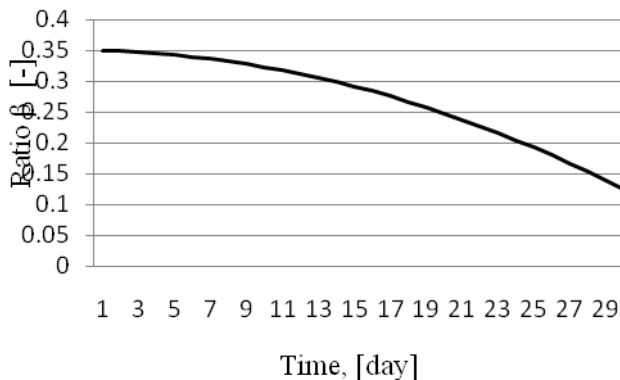


Fig.11. Variation in time of the ratio air volume to reservoir volume,  $\beta$ , due to the air dissolution in water

It may be seen that an exposure of pressurized air to water, during a month, may decrease the value of  $\beta$  from 0,35 to 0,12, in the specific air chamber considered above.

### 4.3 Pipeline protected by Free Air

#### 4.3.1 .Extreme pressures. Method efficiency range

In the third case, when the discharge duct is protected from water hammer by free air deliberately introduced in the pumped water, there was considered an air volume fraction variation between 0,5% and 10 %. These values for the air volume fraction are expressed with respect to the normal atmospheric pressure (101,3 kPa ).

Figures 12-13 present the pressure variation during hydraulic shock, in the case of the discharge duct protected by free air spread into water at different percent values for  $\alpha$ . As the volume fraction of air increases, extreme values of pressure attenuate.

Extreme pressure variation for small values of  $\alpha$  is shown in Fig.12. Comparing with the case of unprotected discharge duct, the maximal pressure decreases from 132mwc to 67mwc and the minimal pressure value increases with about 3 mwc for  $\alpha = 0,5\%$ . Cavitation disappears. This method takes effect even at small amounts of dispersed air.

It may also be noticed that the frequency of pressure oscillation is smaller as the volume fraction of gas is greater. This difference is enhanced at small  $\alpha$  values, as it may be observed in Fig. 12.

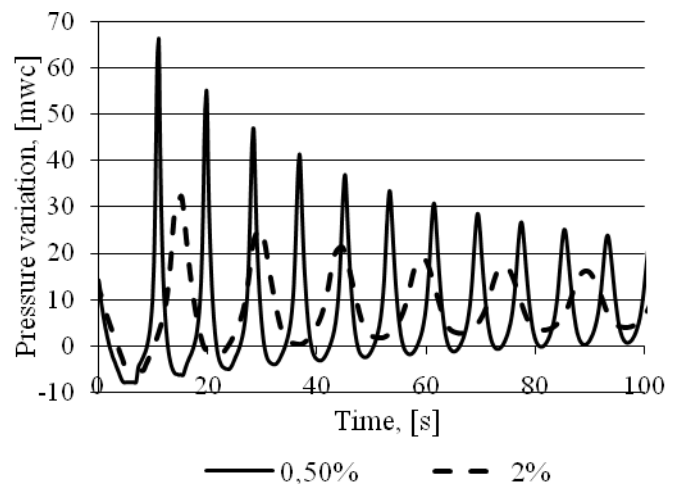


Fig.12. Pressure variation in the case of the discharge duct protected by free air present in water at small values for  $\alpha$ .

As the volume fraction increases, the extreme pressure values attenuate, which means pressure varies in a narrower range.

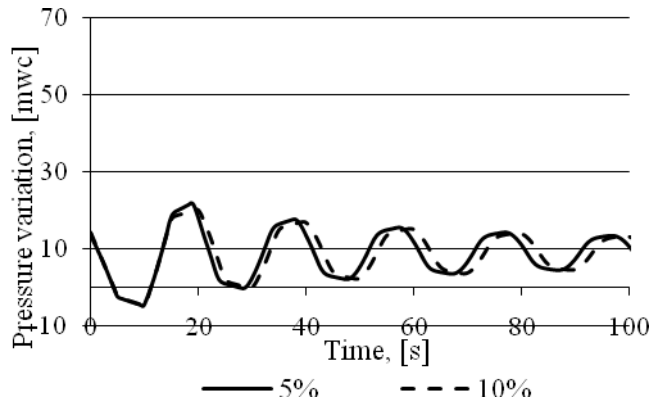


Fig.13. Pressure variation in the case of the discharge duct protected by free air present in water at large values for  $\alpha$ .

If  $\alpha$  rises above 5%, the attenuation of the extreme pressures is slower. The pressure variation curves are very much alike for  $\alpha = 5\% + 10\%$ , as it may be seen in Fig.13.

We may conclude that there is no reason to increase the volume fraction of gas above 5 %.

The simulation of hydraulic shock in a pipeline protected by free air spread homogenously into the pumped water neglected the tendency of air to accumulate in the upper side of the conduit.

**4.3.2. Air Accumulation. Free Air Protection Method Limitations**

The free air may form pockets of gas, according to the inner geometry of the duct and of its fittings. Therefore, the use of free air must be done cautiously, to prevent such accumulations.

The investigation on the air tendency to accumulate in the upper side of the pipeline was carried out on a duct section of 2,2 m in length, Fig.14. This section of duct is equipped with a check valve and an electro valve, both of butterfly type. The inner geometry was simplified, both obturators being considered of ellipsoidal shape.

The study was computationally made using the program *Comsol*, on the above presented section of the discharge duct. We assumed a non homogeneous flow of the two phases inside the horizontal duct, in the presence of the gravitational field [15]. The relative velocity between phases was determined on the basis of the balance of the forces acting on the air bubbles: the drag and the buoyancy force [2], [11].

In Fig.14, the surface colour indicates the air volume fraction field. The regions of light grey represent air accumulations. The arrows indicate the air bubbles velocity at a moment of unsteady flow. The check valve

is completely open, but the electro vae is only partially open.



Fig.14. Biphasic (water-air) non homogeneous flow. Surface colour: air volume fraction field. Arrows: air velocity

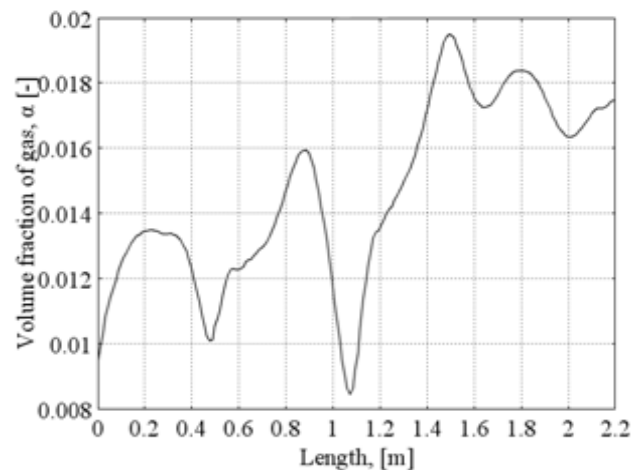


Fig.15. Variation of the air volume fraction. Rotation angle with respect to the duct axis: 30° for both obturators

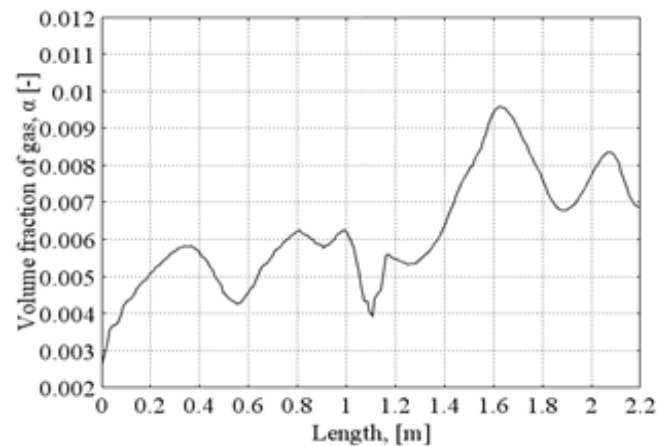


Fig.16 Variation of the air volume fraction. Rotation angle with respect to the duct axis: 0° for the check valve (completely open) and 30° for the electro valve obturator

We computed the variation of the volume fraction of air for different rotation angles between the main axis of each ellipse and the duct axis. Some of these graphs are presented in Fig. 15-18.

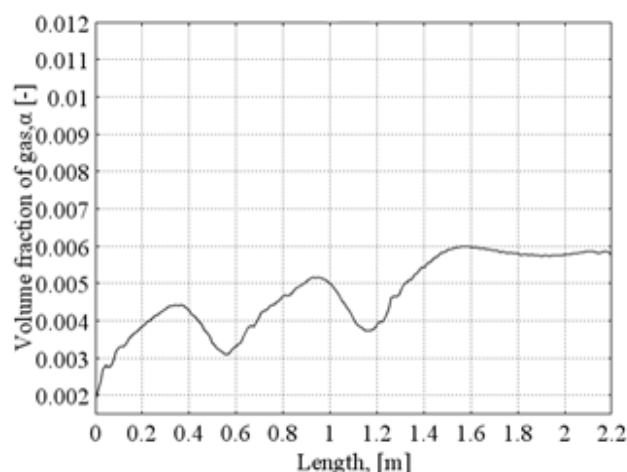


Fig.17. Variation of the air volume fraction. Rotation angle with respect to the duct axis:  $0^\circ$  for both obturators (both valves completely open)

The values of the air volume fraction in these figures are expressed at local pressure.

This sequence of rotation angles illustrates moments during the opening of the electro valve. The biphasic discharge is taken in accordance with the pump's characteristic [3],[4].

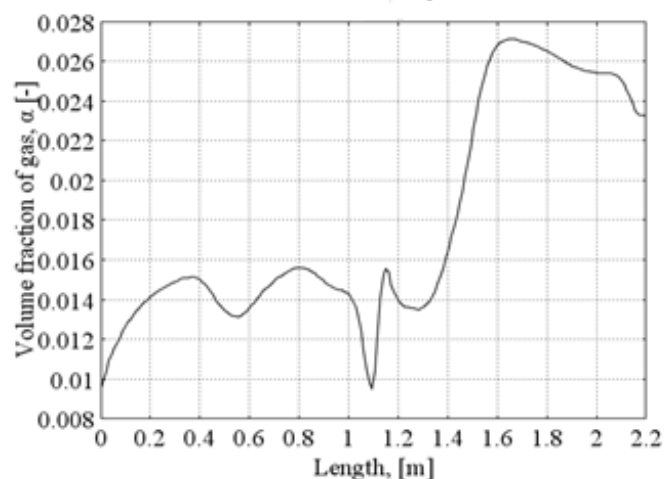


Fig.18. Variation of the air volume fraction. Rotation angle with respect to the duct axis:  $0^\circ$  for the check valve (completely open) and  $45^\circ$  for the electro valve obturator

The maximal value for the air volume fraction, for each of the three cases is recorded immediately downstream the second obturator, in the cross section situated at 1,5-1,6m. The maximum value is reached in

the case both obturators are partially open, Fig.15, when the turbulence is most intense.

When both valves are completely open, Fig. 17, air bubbles are entrained by water and the air volume fraction field tends to be uniform.

Modifications in the field of air volume fraction may occur at any manoeuvre of the electro valve. For example, when the obturator of the electro valve is partially closed at an angle of  $45^\circ$ , Fig.18, the volume fraction of air records the largest value in the considered duct, about 0,027.

In reality, the inner geometry is complex and air is trapped in the upper side of the pipeline, forming pockets.

## 5 Conclusion

Analysing the pressure variation obtained by numerical simulation results the best options to protect the horizontal discharge duct are:

- by the use of air chamber, at  $\beta = 0,35$ ;
- by the use of free air at  $\alpha = 5\%$

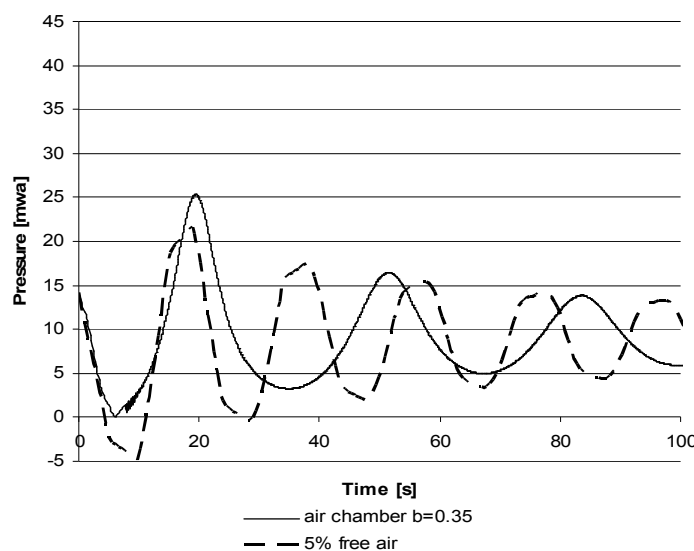


Fig.19.The best variants for protecting the installation by the use of air

The two protection solutions offer almost the same values of maximal pressure, as may be seen in Fig.19. The use of air chamber provides a good protection of the discharge duct, but only if  $\beta \geq 0,3$ . Thus, if accidentally the volume of air in the chamber decreases such as  $\beta \leq 0,12$ , the presence of this chamber becomes a threat to the duct by increasing the maximal pressure during the water hammer. Continuous surveillance of the air volume in the chamber must be imposed as a caution measure.

Free air method seems to be very efficient, but there are a few inconvenient aspects. The air bubbles must be deliberately introduced into the hydraulic circuit, in order to control the volume fraction of gas. The considered circuit is open; therefore a compressor might continuously supply the free air, which results in an increase of electrical power consumption. The use of free air is recommended only in installations where the configuration doesn't allow air to accumulate in different sections of the discharge duct.

We will attempt to extend our study on free air protection method in the case of non homogeneous biphasic movement. Even if the hypothesis of homogeneous flow is enough accurate for the pressure variation determination which interests from the pipe mechanical resistance point of view, the consequences of biphasic movement are complex.

#### References:

- [1] Berna, K.F., Dohmen, J.H., *Numerical and experimental investigation on the flow in a centrifugal pump stage*, Proc. WSEAS Int., Conference on Fluid Mechanics, 2008, pp71-76. [1] Brennen C.E, *Hydraulics of Pumps*, Cambridge University Press, 1985.
- [2] Brennen C.E, *Fundamentals on Multiphase Flow*, Cambridge University Press, 2005.
- [3] Burchiu V, *Pumping Installations*, E.D.P. Bucharest, 1987.
- [4] Constantin, A., *Guidelines for Pumping Stations engineering design*, Ed.Ovidius University Press, Constanta, 2004.
- [5] Constantinescu, Gh, *Contribution on Pressured Hydraulic Installation Protection*, unpublished doctoral thesis, Institutul Politehnic Timișoara, 1983.
- [6] Georgescu, C., *Calculation and operation of the hydraulic networks and their electropumps*, Ed. Matrixrom, Bucharest, 2006.
- [7] Hancu, S., Marin, G., *Hydraulics.Theory and application*, Vol.1, Ed. Cartea Universitara, Bucharest, 2007.
- [8] Hassan,N.M.S., Khan, M.M.K, Rasul, M.G., *A Study of Bubble Trajectory and Drag Coeficient in Water and Non-Newtonian Fluids*, WSEAS Transactions on Fluid Mechanics, Issue 3, Volume5, July 2010, pp.236-245.
- [9] Pinto, J, Afonso, L., Varajao, J, Bentes, I., *Contribution for the vulnerability assessment of water pipe network systems*, WSEAS Transactions on Fluid Mechanics, Issue 3, Volume3, Oct. 2008.
- [10] Popescu, M., Arsenie, D.I., Vlase, P., *Applied Hydraulic Transients for Hydropower Plants and Pumping Stations*, Balkema Publishers, Lisse, Abington, Tokyo, 2003, 2004.
- [11] Roston, G.B., Ascheri, M. E., Martin M.C., Pizarro R., *Void fraction fluctuations in two phase flow: theoretical models*, WSEAS Transactions on Fluid Mechanics, Issue 4, Volume3, Oct. 2008.
- [12] Stoicuta, O., Nan, M.S., Dimitrache, G., Buda, N., Dandea, D.L., *Research tregarding the use of new systems to control fluid flow in pipelines*, WSEAS Transactions on Fluid Mechanics, Issue 3, Volume 5, July 2010.
- [13] Sander, R, *Compilation of Henry's Law Constants for Inorganic and Organic Species of Potential Importance in Environmental Chemistry*, Air Chemistry Department, Max Plank Institute, Mainz, April 1999, pp.3-7.
- [14] Streeter, V.L., Wylie, B. E., *Hydraulic transients*, McGraw – Hill Book Company, New York, 1987.
- [15] \* \* \* *COMSOL MULTIPHYSICS*, [www.comsol.com/products/tutorials](http://www.comsol.com/products/tutorials), 2007.